Materials Advances

ROYAL SOCIETY OF CHEMISTRY

PAPER

View Article Online
View Journal | View Issue

Cite this: *Mater. Adv.*, 2023, 4, 4784

A dynamic hard domain-induced self-healable waterborne poly(urethane/acrylic) hybrid dispersion for 3D printable biomedical scaffolds†

Samiran Morang,[a] Jay Hind Rajput,[b] Anwesha Mukherjee,[c] Atharva Poundarik,[b] Bodhisatwa Das[c] and Niranjan Karak*[a]

Polyurethane (PU) with its efficient self-healing ability and high mechanical properties is highly anticipated but an arduous challenge to achieve. In this study, to create a win–win situation, a new strategy was introduced which is based on the triple synergistic effect of a 'dynamic hard domain', 'multiple hierarchical hydrogen bonding', and 'semi-interpenetrating network (IPN) formation'. The dynamic disulfide bond of 2-APDS and multiple hierarchical hydrogen bonding raised from urea and urethane linkages supplement the healing ability, and concurrently, the polyacrylates and rigid aromatic moiety improve the mechanical properties of the SWPUA films. Owing to the judicious molecular engineering and aforementioned tactic, a series of self-healable waterborne PU/polyacrylic (SWPUA) films were prepared by using bis(2-aminophenyl) disulfide (2-APDS) as the 'dynamic hard domain', monoglyceride of castor oil (MG_{CO}) as a chain extender, glycerol ester of citric acid (GECA) as an internal emulsifier and different acrylate monomers with other desired reactants (polyols/diamines and diisocyanate). The resulting films exhibit good mechanical robustness, high thermal stability, and biodegradability. Notably, a maximum healing efficiency of 82.53% can be achieved within 330 s under microwave exposure (800 W) and the cut films were re-processable at 60 °C under a pressure of 60–80 kg cm^{-2}. Most importantly, the MTT and live/dead assays of mouse fibroblast cell lines (L929) treated with the SWPUA-2 dispersion (up to 30%) confirmed its biocompatibility. Most interestingly, SWPUA-2 can be employed to prepare a SWPUA-2/methacrylate anhydride-modified gelatin (GelMA)/gelatin hybrid ink for the development of 3D printable biomedical scaffolds.

Received 28th August 2023,
Accepted 7th September 2023

DOI: 10.1039/d3ma00607g

rsc.li/materials-advances

Introduction

Waterborne polyurethane (WPU) is one of the sought-after polymers because of its environmentally friendly character and magnificent performance. It has been extensively used in different fields including coatings, inks, and adhesives.[1] But like other polymers, WPUs are also susceptible to damage in byzantine and harsh environments throughout their lifecycle. Premature damage crops up due to the presence of small imperfections or micro-cracks in the material. Some of these cracks are inherent and arduous to repair. This results in catastrophic failure of the material before its desired service life. Nowadays, researchers mimic the renowned natural phenomena of self-healing to resolve these problems.[2] All living organisms can mend minor or major damage by themselves without any external stimuli, which contributes to their longevity. The introduction of self-healing features into WPU is a very enthusiastic field of research. This salient feature greatly enhances the reliability and longevity of WPU. Furthermore, it improves safety in service, decreases raw material consumption, reduces carbon emissions, and above all minimizes maintenance costs. Thus, the ultimate self-healing WPU (SWPU) has become a promising futuristic material having numerous potential applications in the fields of smart coatings, wearable and flexible electronics, and sensors, along with others. A literature survey discloses that self-healing mechanisms can be classified into two broad categories: extrinsic and intrinsic.[3] Extrinsic self-healing involves the dispersion or encapsulation of external healing agents, *e.g.*, reparable monomers, catalysts, and initiators, in the polymer matrix. When cracks or damage occur, the catalysts/initiators initiate/

[a] *Advanced Polymer and Nanomaterial Laboratory (APNL), Department of Chemical Sciences, Tezpur University, Napaam, 784028, Tezpur, Assam, India. E-mail: karakniranjan@gmail.com*
[b] *Department of Metallurgical and Materials Engineering, Indian Institute of Technology Ropar, Punjab 140001, India*
[c] *Biomaterials and Tissue Engineering Lab, Department of Biomedical Engineering, Indian Institute of Technology Ropar, Punjab 140001, India*

† Electronic supplementary information (ESI) available. See DOI: https://doi.org/10.1039/d3ma00607g

facilitate the polymerization of the monomers, and then the crack is repaired. Although this method is trustworthy, healing occurs in a single event, which restricts its popularity. In contrast, intrinsic self-healing occurs in multiple events and is conducive to the polymeric materials being repeatedly repaired. Multiple healing potentialities are developed from dynamic covalent bonds or dynamic non-covalent interactions. Dynamic covalent bonds can be prepared using disulfides, diselenium or ditelluride exchange reaction, Diels–Alder reaction, boronic ester chemistry, triazolinedione chemistry, transesterification, hindered urea bonds, alkoxyamine bonds, transcarbamoylation, and olefin metathesis reaction.[4] Again, non-covalent interactions include hydrogen bonds, metal–ligand coordination bonds, ionic bonds, π–π interactions, and host–guest interactions. It is noteworthy that the favorable conditions (high chain mobility, and exchange of dynamic bonds) for self-healing always conflict with the indispensable conditions (high chain rigidity, intermolecular interaction, and crystallinity) for mechanical strength. So, efficient self-healing and high mechanical strength of WPUs are two contradictory properties. Thus, simultaneous improvement of these two vital properties is always a formidable challenge. Previously, several scientists have proposed ingenious strategies to address this issue. However, the most used strategies include the introduction of an asymmetric alicyclic structure adjacent to an aromatic disulfide molecule,[5] a dynamic hard domain,[6] synergistic triple dynamic bonds,[7] *etc.* Shi and co-workers prepared efficient self-healable WPU by introducing a novel visible-light-induced dynamic covalent bond, which was developed from aromatic Schiff base (ASB) bonds. The final WPU was healable under a commercial LED lamp within 24 hours (~25 °C) with a healing efficiency of 83.8% and it exhibited desirable mechanical strength (tensile strength of 14.32 MPa). They proposed that the ultimate healing originated from the imine metathesis of the ASB bond and was triggered by visible light and H-bond interactions between urethane groups.[8] Wei *et al.* introduced a mechano-responsive tactic, known as strain-induced crystallization, to synthesize room-temperature self-healing polyurethane (PU) exhibiting outstanding tensile strength, toughness, and fracture energy values of 29.0 MPa, 121.8 MJ m^{-3}, and 104.1 kJ m^{-2}, respectively. They reported that the high performance is the result of hierarchical H-bonding interactions and rational optimization of the effective soft segment.[9] In the same year, Zhang and co-workers employed dithiodiphenylamine, a rigid structure, to prepare a multi-functional castor oil-based self-healing WPU showing high tensile strength, processability, and a tunable dual-to-quadruple shape memory effect.[10] Again, Zhang *et al.* prepared a self-healing PU by introducing dynamic covalent C–N bonds formed by an aza-Michael addition between 2,6-di-*t*butyl-7-phenyl-*p*-quinone methide and secondary amine nucleophiles.[11] Recently, a bionic self-healing PU elastomer was prepared by Wand and co-workers using poly(tetramethylene ether glycol), hexamethylene diisocyanate (HMDA), and 1,8-*p*-menthane diamine or 1,8-diamino-*p*-menthane (MD) and bis((2-hydroxyethyl)disulfide) (SS) as chain extenders.[12] They proposed that the H-bonded urea groups obtained from the reaction between the MD amino groups and isocyanate enhanced the mechanical properties. Simultaneously, the stiff ring structure of MD helps the breakdown of disulfide bonds. The resulting MD-PU-SS elastomer exhibits a high tensile strength and fracture energy, good healing efficiency, and recyclability. Again, Rong *et al.* prepared a series of self-healable WPU with the synergistic reversible units of aliphatic disulfide bonds and quadruple hydrogen bonding originated from bis(2-hydroxyethyl) disulfide, (2-HEDS) and ureidopyrimidone (UPy), respectively.[13] Applying the same strategy, Liu and his co-workers also developed another self-healable WPU with wear resistant and recyclable attributes.[14] Wu *et al.* prepared a self-healing hybrid polyurethane acrylate *via* solution polymerization techniques and reported that a maximum of 94% healing efficiency can be achieved by heating at 95 °C for 4 h.[15] Recently, Sun and his co-workers developed a series of micro-cracked self-healable WPU/polyacrylate composites by varying the amount of 2-HEDS on the polymeric chain. The results showed that all of the prepared SWPUAs have excellent dispersion stability, thermal stability, self-healing efficiency and certain hydrophobic capacity.[16]

However, none of these PUs used toxic organic solvents in their complicated synthetic procedures, and tests for biodegradability and biocompatibility were not reported. Concerning environment benignity, in this study, a series of organic solvent-free, and surfactant-free self-healable WPU/polyacrylic (SWPUA) dispersions were synthesized using 2-APDS as the 'dynamic hard domain' along with other required reactants and different acrylate monomers. Here, acrylate monomers were used as the diluent to the polymerization medium at the beginning and polymerized *via* the seeded mini-emulsion polymerization technique at the final stage to obtain the desired dispersion. Remarkably, the resultant dispersion is highly stable for up to six months (zeta potential −47.1 to −60.4) and all SWPUA films exhibited good healing efficiency, mechanical robustness, thermal re-processability, and biodegradability. Most importantly, the MTT assay and live/dead assay of mouse fibroblast cell lines (L929) treated with the SWPUA-2 dispersion confirmed its biocompatibility. Furthermore, we have explored the 3D printability of the SWPUA-2 dispersion by preparing a SWPUA-2/methacrylate anhydride-modified gelatin (GelMA)/gelatin hybrid ink, which was used for the development of a biomedical scaffold and 3D articles.

Experimental section

Materials

Isophorone diisocyanate, (Sigma Aldrich; 98%), poly(ε-caprolactone) diol (ε-PCL, Sigma Aldrich, M_n = 2000 g mol^{-1}), 2,2-bis(hydroxymethyl) propionic acid (DMPA, Sigma Aldrich; 98%), bis(2-aminophenyl) disulfide (2-APDS, Sigma Aldrich; 97%), 1,6-diaminohexane (HMDA, Sigma Aldrich; 98%), citric acid (Sigma Aldrich; ≥99.5%), glycerol (Sigma Aldrich; ≥99.5%), castor oil (Sigma Aldrich), triethyl amine (TEA, Sigma Aldrich; ≥99.5%), potassium persulfate (KPS, Sigma Aldrich; ≥99%), *para* toluene

sulphonic acid (*p*-TSA, Sigma Aldrich), dibutyltin dilaurate (DBTDL, Sigma Aldrich; 95%), and *N*,*N*-dimethylacetamide were used as received. Technical-grade monomers, methyl methacrylate (MMA, Sigma Aldrich; 99%), butyl acrylate (BA, Sigma Aldrich; ≥99%), 2-hydroxyethyl methacrylate (HEMA, Sigma Aldrich; ≥99%), and glycidyl methacrylate (GMA, Sigma Aldrich; ≥97%) were used without further purification. Double-deionized water was used throughout the work.

Preparation of 4-(2,3-dihydroxypropoxy)-2-(2-(2,3-dihydroxypropoxy)-2-oxoethyl)-2-hydroxy-4-oxobutanoic acid or glycerol ester of citric acid (GECA)

GECA was prepared by the esterification reaction of 12.5 mM of citric acid and 25 mM of glycerol catalyzed by *p*-TSA (0.5 wt% of citric acid), as reported earlier.[17]

Preparation of the monoglyceride of castor oil (MG_{CO})

The MG_{CO} was prepared by a previously reported process and a brief description is added in the (ESI†).[18]

Synthesis of SWPUA dispersions

Fig. 1 summarizes the synthesis route of the SWPUA dispersion. The reaction setup comprises a 100 mL three-neck round bottom flask equipped with a nitrogen inlet, a thermometer, a septum, and a Teflon blade stirrer. The formulations of various PU-acrylates (PUAs) are presented in Table S1 (ESI†). For the synthesis of the NCO-terminated prepolymer, ε-PCL_{2000} (1 mM), DMPA (1.5 mM), IPDI (3 mM), DBTDL (0.05 wt% of PU), and 25% of the acrylate monomers were added into the round bottom flask. The prepolymer formation was confirmed by FTIR spectral analyses.

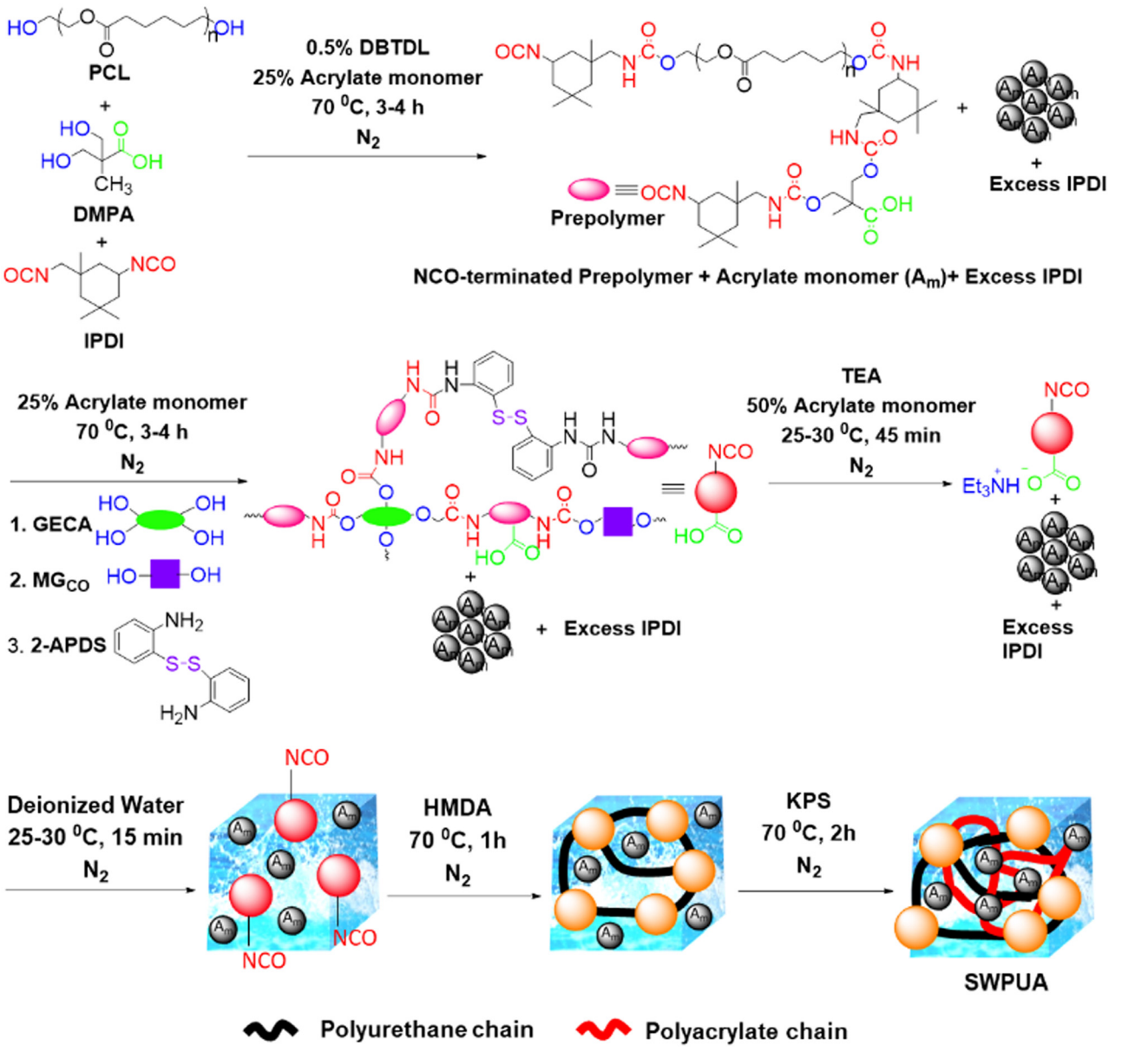

Fig. 1 The representative reaction scheme for the synthesis of SWPUA.

Then, 2-APDS (0.80 mM), GECA (0.375 mM), MG_{CO} (1 mM), 25% of the acrylate monomers, and the remaining IPDI (3.65 mM) were added to the mixture and reacted for 3–4 h at 70 °C. Then, the reaction mixture was cooled to 25–30 °C, and TEA (2.81 mM) and the remaining 50% of the acrylate monomers were added to the mixture and stirred for 45 min at the same condition to neutralize the carboxylic groups of GECA and DMPA. Subsequently, the aqueous dispersion was prepared by adding double de-ionized water to the prepolymer–monomer mixture at the same temperature within 15 min under high agitation (750 rpm). Then, HMDA (0.35 mM) was added, and the reaction was continued for 1 h at 70 °C. Finally, the acrylate monomers were polymerized *via* a free radical chain-growth polymerization mechanism. The reaction was performed for 2 h at 70 °C by adding KPS solution in water (1 g) in a single shot. Finally, a stable whitish SWPUA dispersion was obtained.

Preparation of the films

The synthesized SWPUA dispersions were cast on different flat surfaces for different tests and analyses. The films cast on metal steel plates (150 mm × 50 mm × 5 mm) were used for the impact resistance study, those on glass slides (80 mm × 30 mm × 10 mm) were used for scratch hardness tests, and those on Teflon sheets were used for various measurements including tensile strength, elongation, and toughness. All of the films were dried at room temperature for 2 days followed by vacuum drying at an elevated temperature to remove the remaining solvent and kept in a desiccator. All of the films were kept under ambient conditions for 2 days before their testing and analyses.

General characterization

The methods and techniques used to characterize the SWPUA dispersions and films are demonstrated below. All of the tests and evaluations were carried out under ambient conditions unless otherwise mentioned.

Structural analysis

The FTIR spectra of the NCO-terminated prepolymer and all of the SWPUAs were recorded by a Nicolet Impact 410 FTIR spectrometer (Madison, USA) from 500 to 4000 cm^{-1} using KBr pellets. The ^{1}H and ^{13}C NMR spectra of SWPUA-2 were recorded by a Bruker Biospin AG 500 MHz NMR spectrometer (Model-Avance III HDX, USA) using DMSO-d_6 as the solvent and TMS as the reference.

Physical property measurement

The average particle size of the SWPUA dispersions was measured by a NanoPlus dynamic light scattering system (DLS, Particulate System, USA) and investigated by Transmission Electron Microscopy (HR-TEM, 300 kV, Tecnai G2, F30, FEI, USA). The static angle for each polymeric film was calculated by the sessile-drop method using a DropMaster Automatic Contact Angle Meter (model-DMs-401, Kyowa Interface Science Co. Ltd, Japan). Gel Permeation Chromatography (GPC, Waters, UK) was used to determine the average molecular weight (Mw and Mn) and polydispersity index (PDI) of the synthesized SWPUAs. Linear polystyrene was taken as the standard polymer. Furthermore, the transmittance of all SWPUA films was measured by a UV-VIS spectrophotometer (Model-Evolution 300, Thermo Fischer Scientific, USA) from 200 nm to 800 nm.

Thermal analysis

Thermal analysis (TGA) was carried out in a TGA-4000 (PerkinElmer, USA) thermal analyzer from 30 °C to 700 °C at a heating rate of 10 °C min^{-1} and using N_2 as the purged gas. Again, DSC-6000 (PerkinElmer, USA) equipped with an intercooler system was used to determine the glass transition temperature of the SWPUAs. The calorimetric test was performed in three steps in order, heating, cooling, and heating in the range of −70– to 160 °C at a heating rate of 10 °C min^{-1} under a N_2 atmosphere.

Mechanical performance test

SWPUA films were cut into a rectangular specimen of 5 cm × 1 cm (length × width) and a Universal Testing Machine (UTM, model-WDW-10, Jinan, China) with a 0.5 kN load cell was employed to measure the tensile strength and elongation at break. The rate of displacement was 20 mm min^{-1}. The scratch hardness test was performed by using a scratch hardness tester (model-705, Sheen Instrument Limited, UK) with different weights at a travel speed of 50 mm s^{-1}.

Self-healing test

The self-healing ability of the SWPUAs and SWPU were evaluated both quantitatively and qualitatively. To investigate the healing performance, rectangular specimens of ∼40 mm × 10 mm × 0.55 mm (length × width × thickness) were cut in a transverse direction (length ∼ 5 mm) by a sharp razor blade. The damaged area was healed using a domestic microwave oven at different powers (600 W, 700 W, and 800 W). The healed and unhealed areas were tracked using an optical microscope. Weightlifting and stretching tests were also performed after healing and videos of both tests are provided in the ESI.† In this study, the healing efficiency was defined as the ratio of restored tensile strength after healing to the original tensile strength and calculated according to eqn (1). At least three healed specimens of each sample were analyzed by the tensile test.

$$\eta_h = (\sigma_h/\sigma_o) \times 100 \quad (1)$$

Here, σ_o is the tensile strength of the pristine film, and σ_h is the tensile strength of the healed film.

Re-processability test

To investigate the reprocessing performance, the films were cut into small pieces with the dimensions of ∼2.5 mm × 2.5 mm × 0.55 mm (length × width × thickness). The pieces were reprocessed by hot-pressing. The change in the tensile strength was evaluated after the physical reprocessing. The recycling efficiency is calculated according to eqn (2).

$$\eta_h = (\sigma_r/\sigma_o) \times 100 \quad (2)$$

Here, σ_o is the tensile strength of the original film, and σ_r is the tensile strength of the reprocessed film.

Cell culture and maintenance

The cytotoxicity and cytocompatibility of the SWPUA-2 polymer were studied against mouse fibroblast cell lines (L929), as these cells are responsible for extracellular matrix production. The cells were maintained and cultivated following the standard protocol. Briefly, the cells were grown in a sterile incubator at 37 °C with 5% CO_2 and >90% humidity. After that, the cells were taken out and allowed to reach 80–90% confluence in high glucose DMEM growth media (Gibco, USA) containing 10% fetal bovine serum (FBS, Gibco, USA) and 1% antibiotic–antimycotic solution (Himedia, India). After removing the media, sterile PBS was used to wash the cells. The cells were then trypsinized and moved to a new flask with fresh growth medium.

In Vitro cytotoxicity evaluation

Cell proliferation analysis by MTT assay. An *in vitro* cytocompatibility assay was carried out using L929 *via* a cell viability [MTT (3-(4,5-dimethylthiazol-2-yl)-2,5-diphenyltetrazolium bromide)] assay for a period of 3 days. Different concentrations of SWPUA-2 solution (10%, 20%, and 30%) were sterilized for 1 h under exposure to UV radiation. A control sample was prepared without SWPUA-2. Then, 100 μL of a cell suspension of 10^5 cells per ml with DMEM complete medium was dispensed into the peripheral wells of a 96-well tissue culture microliter plate. After 24 h and 72 h of incubation, the medium was removed and replaced by fresh medium. Then, MTT solution was added to the samples along with the control and incubated for 3 h. Then, DMSO was added to each well and mixed well to solubilize the formazan crystals. The relative reduction in cell viability in comparison to the untreated control group was then measured at 570 nm using eqn (3). Experiments were repeated three times.

$$\text{Cell viability (\%)} = (\text{Mean optical density}/\text{Control optical density}) \times 100 \quad (3)$$

Live/dead assay

Using a live/dead assay following the manufacturer's instructions, cell viability was assessed after 3 days of seeding.

Then, different concentrations of SWPUA-2 samples were washed with PBS and incubated with calcein AM (4 mM, Merck, Germany) for staining live cells and ethidium bromide for staining dead cells (2 mM, Himedia, India) with serum-free DMEM for 45 min at 37 °C in a humidified incubator. Post-staining, the samples and control were washed with PBS and the cells were imaged using a Leica fluorescence microscope (E_x = 501 nm; E_m = 521 nm and E_x = 301 nm; E_m = 603 nm for calcein AM and ethidium bromide). Experiments were performed in triplicate.

Preparation of SWPUA-2/GelMA/gelatin-based scaffolds using a 3D bio-printer

By combining gelatin with modified gelatin (GelMA) following a well-studied method and SWPUA-2 at appropriate concentrations, an ink was prepared. After that the scaffolds were fabricated for biomedical applications. The GelMA was synthesized by adopting a previously reported synthesis method;[19] 0.5% w/v Irgacure 2959 (photo-crosslinker) solution was prepared in Dulbecco's phosphate buffered saline (DPBS)[20] and 20% w/v GelMA was added to obtain the final solution. An ANGA PRO 3D having a twin extruder bio-printer (ALFATEK SYSTEMS) was used to print the ink {(GelMA/SWPUA-2)/Gelatin}. To get good mechanical stability, a photo crosslinker (Irgacure 2959) was used, which crosslinked to GelMA. A prepared solution of gelatin (20% w/v) that was added into the ink helped improve the printability and compensated for the compromised printability by adding GelMA. A luer syringe attached with a 22 G conical tapered tip was utilized for making distinct scaffolds. The ink solution was kept for a few min at ambient temperature until the ink showed printability, having partially solidified and viscous characteristics. A cuboid design (2.5 cm × 2.5 cm ×1 cm) was created using the SOLIDWORKS 2021 student version design software in a.amf format. The.amf file was sliced and converted into the G. Code format with optimized process parameters using Cura_14.09 software. The G. Code file was loaded on Melzi-Mendel software, then the printer was run to construct the scaffolds on a Petri-dish.

Biodegradation test

The biodegradation of SWPUA was studied through a soil burial method. A calculated amount of each sample was put into a disposable teacup and buried inside soil 20–30 cm deep in an open area with Latitude-26°41′56.7708″ and Longitude-92°50′2.8896″ for 120 days. The weight loss was calculated and the changes in the surface morphology of each sample were evaluated using a scanning electron microscope (SEM, Model-JSM 6390LV, Jeol, Japan).

Results and discussion

Synthesis and characterization of SWPUA dispersions and films

It is well-known that healing efficiency is always associated with good chain mobility, which opposes high mechanical strength. To create a win–win situation, the rigidly structured 2-APDS and different acrylates were incorporated into the WPU system *via* a seed mini-emulsion polymerization. As shown in Fig. 1, a series of SWPUA hybrid dispersions with different acrylates (Table S1, ESI†) were synthesized in the absence of solvent by step-growth and free radical chain-growth polymerization techniques, simultaneously. Here, HMDA is more nucleophilic than 2-HEMA towards NCO groups of IPDI. The chemical structure of the SWPUAs was confirmed by FTIR and NMR spectral analyses as discussed below. Fig. 2(a) and (b) show the absorption peaks of various functional groups present in the synthesized polymer dispersions and prepolymer (SWPUA-2). Notably, the characteristic absorption peaks of the –NCO and –OH groups were absent near 2267 cm^{-1} and 3500 cm^{-1}, respectively, which confirmed that the –NCO group must be converted to either urethane or a urea unit. A single peak of the –NH group was observed near 3400 cm^{-1}. The characteristic peak at

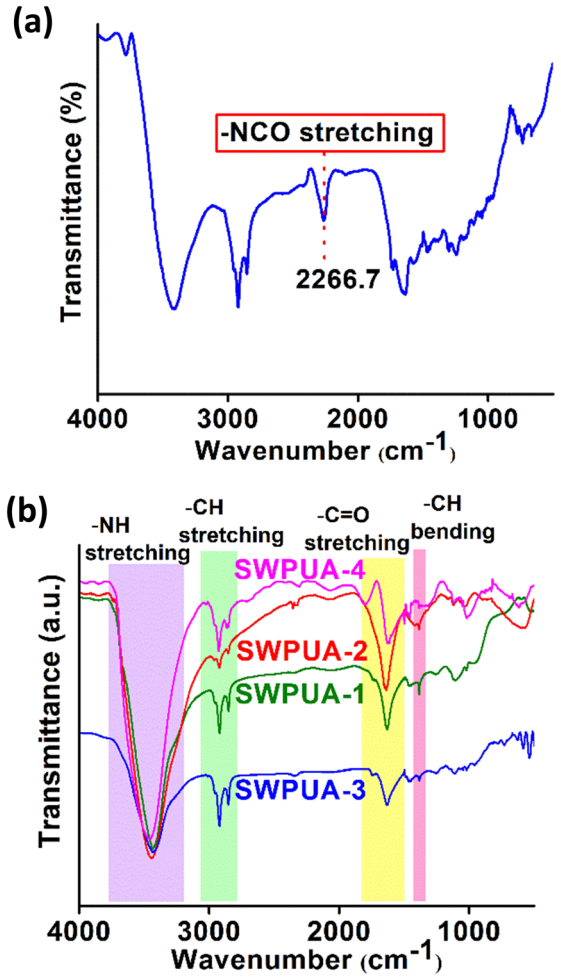

Fig. 2 (a) FTIR spectrum of the prepolymer of SWPUA-2 and (b) FTIR spectra the SWPUAs.

2850 cm^{-1} and 2928 cm^{-1} can be assigned to the symmetric and asymmetric stretching vibrations of the –CH bond, respectively. The stretching vibration of the C═O group was observed at 1641 cm^{-1}. The peaks at 1106 cm^{-1} and 1244 cm^{-1} can be assigned to symmetric and asymmetric stretching vibrations of the C–O–C group. Furthermore, the small band near 1461 cm^{-1} corresponds to the N–H bending vibration. These results suggested that a urethane linkage had been formed. Moreover, Fig. S1 (ESI†) demonstrates the FTIR spectra of SWPUA-4, MMA monomer, and 2-HEMA monomer. Finally, the proposed structure of the SWPUA-2 was confirmed by ^{1}H and ^{13}C NMR spectral analyses. The ^{1}H NMR spectrum of SWPUA-2 is shown in Fig. 3(a). In the ^{1}H spectrum, the three peaks at 0.88 ppm (a), 1.06 ppm (b), and 1.30 ppm (c) correspond to the methyl protons present in the acrylates and IPDI moieties of the PU. The peaks at 1.38 ppm (d) and 1.65 ppm (e) correspond to the γ and β methylene protons of the PCL units, respectively. The α-methylene proton of the ester linkage can be found at 2.31 ppm (f). The peaks at 2.92 ppm (g) and 4.05 ppm (h) can be assigned to the α-methylene proton present next to the N-atom and O-atom of the carbamate group, respectively. The proton attached to the N-atom of the primary and secondary isocyanate group was observed at 6.58 ppm (i) and 6.72 ppm (j), respectively. Thus, the data of the ^{1}H NMR spectrum support the probable chemical structure of SWPUA-2. The structure was further confirmed by the ^{13}C NMR spectral analysis. The ^{13}C NMR spectrum of SWPUA-2 is shown in Fig. 3(b). The peak at 14 ppm (a) can be assigned to the terminal methyl carbon present in the MG_{CO} unit of the SWPUA-2. The two types of methyl carbon available in the IPDI moiety appeared at 25.43 ppm (d) and 34.12 ppm (f). The α, β, and γ-methylene carbons concerning the carbamate group were observed at 22.50 ppm (c), 28.34 ppm (e), and 64.01 ppm (g), respectively. A small peak at 71.53 ppm (h) can be assigned to the mid-carbon of the glycerol moiety. Furthermore, the carbonyl carbons present in the carbamate group and the ester groups were found at 150.36 ppm (i) and 173.36 ppm (j), respectively. Thus, all of the peaks support the expected structure of the newly synthesized SWPUA-2.

Physical properties of the SWPUA dispersions and films

As shown in Fig. S2 (ESI†), the solubility test reveals that all SWPUAs were soluble in polar solvents such as THF, DMF, and DMSO, but insoluble in non-polar solvents like hexane, toluene, and xylene. This is because the synthesized polymer contains different polar functional groups such as carbamate groups, ester groups, and carboxylic acids on its surface, which

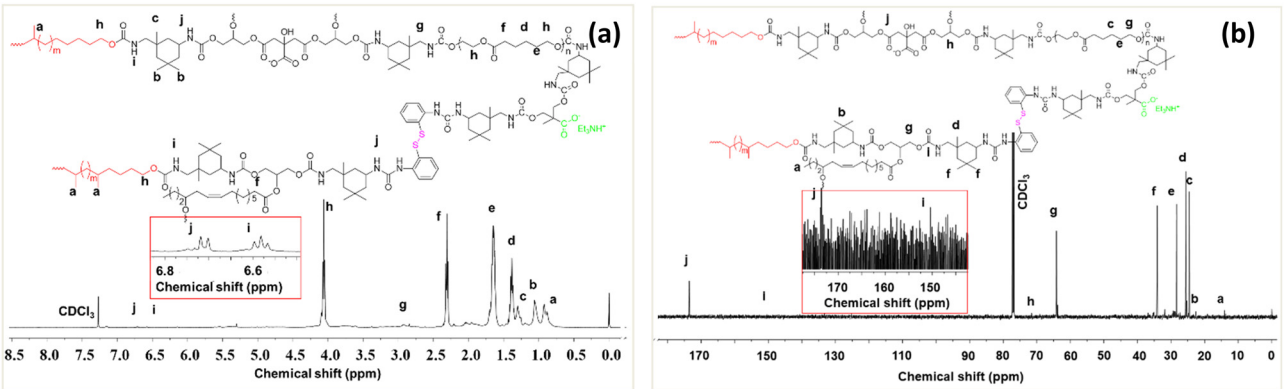

Fig. 3 (a) ^{1}H NMR spectrum and (b) ^{13}C NMR spectrum of SWPUA-2.

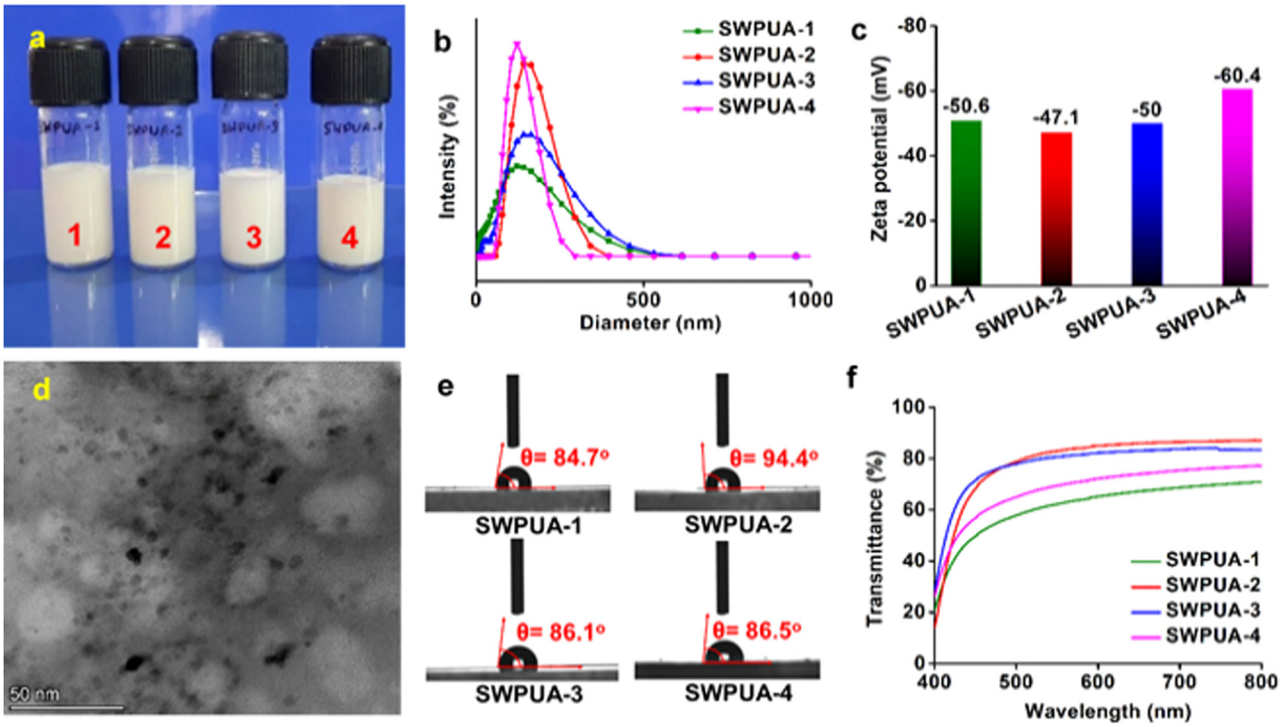

Fig. 4 (a) Digital photos of the SWPUA dispersions, (b) particle size distribution, (c) zeta potential (mV) of the SWPUA dispersions, (d) TEM image of the SWPUA-2 dispersion, (e) contact angle, and (f) transmittance (%) spectra of the SWPUA films.

help the polymer chain to disperse in polar solvents. The average particle size and zeta potential of the SWPUAs are tabulated in Table S2 (ESI†). The results show that the particle sizes of SWPUA-1, SWPUA-2, SWPUA-3, and SWPUA-4 were 105.1 nm, 135 nm, 109.6 nm, and 115 nm, respectively. The digital images of all SWPUAs, the TEM image of SWPUA-2, and the particle size distribution curves are shown in Fig. 4(a). Importantly, the particle size of the dispersion is related to the weight percentage of the emulsifier and cross-linker (functionality, $f \geq 3$) used.[21] A higher content of cross-linker results in a large particle size because of a high degree of branch formation. But a higher amount of emulsifier produces a high surface charge density in the polymeric chain, generating electrostatic repulsion. This repulsion does not allow the polymeric particles to aggregate, resulting in a small particle size distribution. As all compositions contain the same amount of DMPA (act as an internal emulsifier) and GECA (act as a bio-based internal emulsifier and cross-linker), the respective particle sizes do not deviate very much from each other. However, it can be seen clearly that SWPUA-2 possesses small particles as compared to the other compositions, which can be attributed to the proper grafting of 2-HEMA to the PU backbone *via* the urethane linkage.[22] Thus, the narrow particle size distribution (Fig. 4(b)), zeta potential (lower than −47 mV) (Fig. 4(c) and Fig. S3, ESI†), and TEM image (Fig. 4(d)) support the high stability of the resultant SWPUA dispersions. Fig. 4(e) shows the water contact angle of SWPUA with different acrylate contents and the values are summarized in Table S2 (ESI†). The hydrophobic properties of SWPUA depend on the content of the internal emulsifier, polar group, and hydrophobic moieties. Generally, waterborne systems exhibit contact angles smaller than 90° because of hydrophilic groups. However, the contact angle of SWPUA-2 was 94.4°, which can be attributed to the successful grafting of the acrylate unit (2-HEMA) with the WPU matrix to form a new hydrophobic semi-interpenetrating polymer network.[19] Furthermore, the average molecular weight of all SWPUAs was determined by Gel Permeation Chromatography (GPC) analysis. It was observed that the weight-average molecular weight (M_w, g mol^{-1}) and number-average molecular weight (M_n, g mol^{-1}) of SWPUA-1, SWPUA-2, SWPUA-3, and SWPUA-4 were 173 265 and 106 876, 146 783 and 91 281, 151 605 and 91 996, and 150 184 and 92 194, respectively (Fig. S4, ESI†). The polydispersity index (PDI) values were observed in the range of 1.607–1.647. The low PDI values correspond to the uniform polymeric chain, resulting in well-defined thermo-mechanical and self-healing properties.[23,24] Furthermore, the visible light transmittance values of SWPUA-1, SWPUA-2, SWPUA-3, and SWPUA-4 were 71%, 87%, 83%, and 77%, respectively, as shown in Fig. 4(f). The high transparency can be attributed to the small particle size distribution (Fig. 4(b) and Table S2, ESI†) and poor crystallinity of the SWPUA films.[25]

Thermal properties of the SWPUA films.

The thermal properties of all of the films were investigated from the TGA and DSC analyses as shown in Fig. 5(a)–(c) and summarized in Table S3 (ESI†). The results showed that all the compositions exhibited good thermal stability. Generally, the main factors responsible for the thermal stabilities are

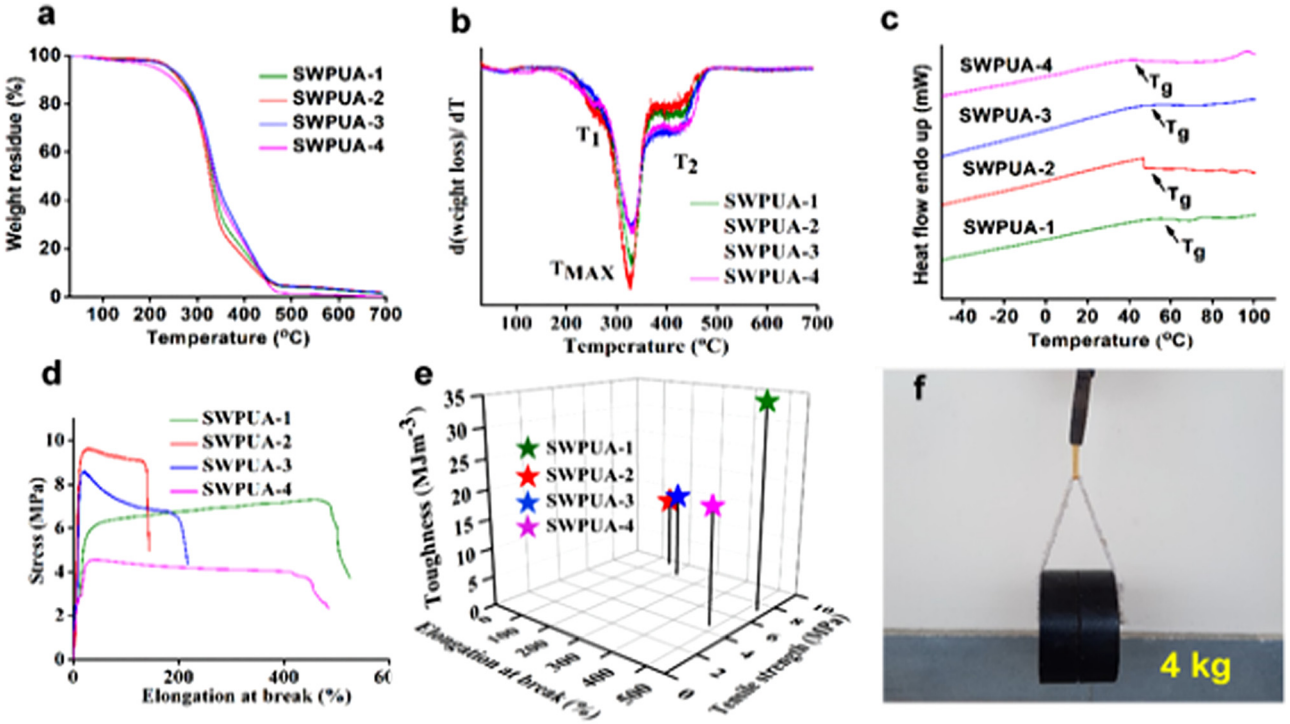

Fig. 5 (a) TGA curves, (b) DTG curves, (c) DSC curves, (d) stress–strain profiles and (e) toughness of the SWPUAs, and (f) a photo showing a load of 4 kg lifted using an SWPUA-2 film.

the degree of polymerization, *i.e.*, the number of urethane linkages, the ratio of hard segments to soft segments, the number of aromatic moieties, the molecular weight distribution, and the extent of physico-chemical cross-linking.[26] The TGA and DTG curves demonstrated that all of the SWPUAs and SWPU undergo three-step thermal degradations and the corresponding temperatures are denoted as T_1, T_{MAX}, and T_2. A similar thermal degradation pattern of WPUA was reported by Qiu and co-workers.[27] The first step degradation (T_1) was observed in the range of 235.27–256.85 °C. This step can be attributed to the degradation of weak dynamic disulfide bonds and the long aliphatic hydrocarbon chain of MG_{CO}. Noticeably, a great extent of mass loss was found in the second step of thermal degradation (T_{MAX}) in the range of 328.45–330.39 °C because of the deterioration of relatively more thermostable moieties like the carbamate group, ester linkages, and IPDI moieties. Then, the final step of degradation (T_2 > 415 °C) corresponds to the most thermostable units, including the aromatic ring of 2-APDS, and the carbon char and ash formation process. GECA has a great effect on the thermal stability of all films. It contains two primary hydroxyl groups and two secondary hydroxyl groups, which cause a high degree of chemical cross-linking, resulting in high thermal stability. Additionally, the TGA curve of ε-PCL_{2000} is also shown in Fig. S5 (ESI†) to show the change in thermal stability before SWPUA film formation. The one step degradation can be attributed to the thermal degradation of the ester groups. Moreover, Fig. 5(c) shows the DSC curves of all SWPUAs. The glass transition temperatures (T_g) of SWPUA-1, SWPUA-2, SWPUA-3, and SWPUA-4 were 54.38 °C, 46.89 °C, 47.14 °C, and 39.38 °C, respectively.

Mechanical performances of the SWPUA films

The mechanical properties of all of the SWPUAs were studied and the values are tabulated in Table S3 (ESI†). The stress–strain profiles of SWPUA are shown in Fig. 5(d). It was observed that all films exhibited moderate tensile strength and average elongation at break. Here, the moderate tensile strength of the SWPUA films can be accredited to high molar mass, multiple hydrogen bonds, the rigidly structured benzene ring, and the cycloaliphatic IPDI ring. The multiple hydrogen bonding develops physical cross-linking in the PU matrix. The MG_{CO} contains three hydroxyl groups (two primary and one secondary), while GECA contains four hydroxyl groups (two primary and two secondary). So, crosslinking is sufficient to cause high mechanical strength. Additionally, the grafting of the acrylate monomer *via* urethane bond formation and semi-interpenetrating network formation *via* free radical polymerization provides a greater increment in the final tensile strength.[28] The grafted polymer, *i.e.*, SWPUA-2, showed the highest tensile strength and very low elongation at break, as expected. The tensile strength and elongation of SWPUA-2 were 5.79 ± 0.1 MPa and 121 ± 1%, respectively. The high tensile strength and average elongation caused the polymeric film to be mechanically tough. In this study, the toughness was measured by integrating the area under the stress–strain curve (Fig. 5(e)). As shown in Fig. 5(f), it has been observed that an SWPUA-2 film could be used to lift a load of 4 kg, which also supports its

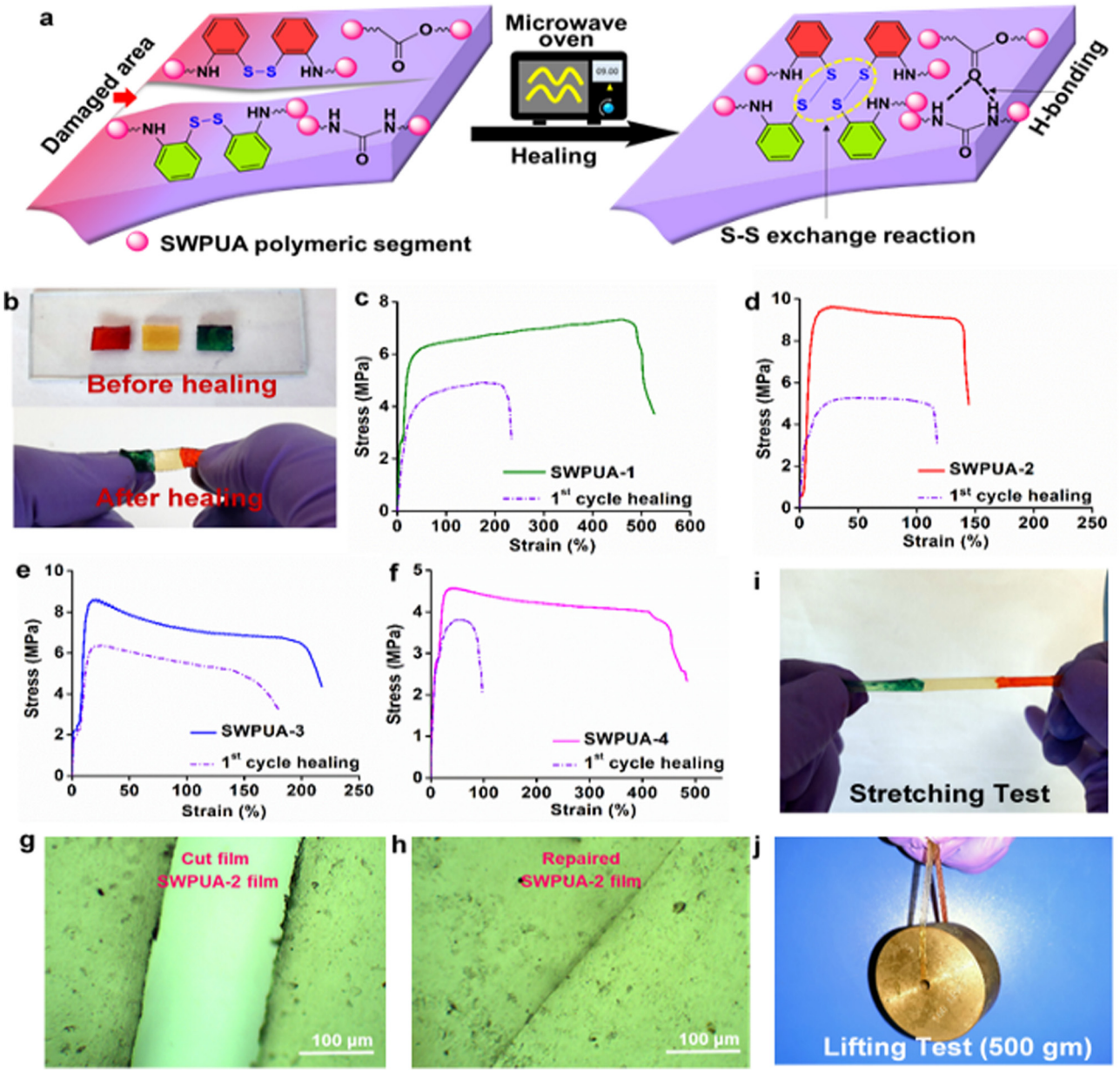

Fig. 6 (a) Possible healing mechanism, (b) three pieces of cut film before healing and the joined film after healing at 800 W for 330 s, (c)–(f) stress–strain profiles of the SWPUA film after the 1st cycle of healing at 800 W for 330 s, (g) and (h) optical microscopic images of the cracked and healed films (SWPUA-2), and (i) and (j) stretching and weight-lifting test after healing of SWPUA-2.

high toughness. Furthermore, the scratch hardness of all SWPUAs was found to be good, which can be attributed to the formation of a semi-interpenetrating polymer and good tensile strength.

Self-healing and re-processability performances of SWPUA films.

The healing efficiency of all SWPUAs was studied quantitatively by evaluating the change in the mechanical strength using UTM. All original samples were cut in the transverse direction with a length and thickness of 5 mm and 0.55 mm, respectively, and then put inside the microwave oven for the specified power and time until completely healed, and the results are summarized in Table S4 (ESI†). To investigate the effect of the acrylate moiety on the healing efficiency of the resultant polymer, various acrylates were incorporated into the WPU matrix. The plausible self-healing mechanism is shown in Fig. 6(a). Then, Fig. 6(c) demonstrates the changes in the stress–strain curves of the original films and the healed films, and the results are tabulated in Table S5 (ESI†). It was observed that the tensile strength and the elongation at break of the pristine sample SWPUA-2 were 9.56 ± 0.3 MPa. But the value was changed to 5.30 ± 0.2 MPa after the first time of healing at 800 W for 330 s, which indicates an efficiency of 55.44%.[29] The healing process

involves various steps such as segmental surface rearrangement, surface approach, wetting, diffusion, and randomization.[30] Different polar groups present on the damaged surface absorbed the necessary energy from the microwave radiation, which helped to oscillate their dipoles. This oscillation generates the rapid Brownian motion of the soft segment, which leads to molecular chain diffusion below the melting temperature (T_m). In the present study, the healing process was intrinsically triggered by multiple hydrogen bonding and disulfide metathesis in the PU matrix. The metathesis can be considered to be a radical-mediated reaction in which homolytic cleavage of the disulfide bond occurs to create new sulfur-based radicals.[31] Finally, these radicals participate in new disulfide bond formation (low activation energy, E_a of 20–50 kJ mol^{-1}) assisted by microwave radiation to heal the fractured surfaces.[32] It has been observed that there is no significant change in the healing efficiency of the final polymer due to any acrylate group. So, it can be concluded that the healing ability is raised because of the presence of polar groups (especially hydrogen bonds) and dynamic disulfide interchange reactions. Notably, in the present study, we have only disulfide bonds as the dynamic segment along with a very small amount of urea linkages. So, the healing ability was developed due to the presence of a dynamic hard domain, *i.e.* 2-APDS. To establish the same, we tried to heal a poly(urethane/acrylic) (PUA) film without disulfide bonds under the same conditions as in the case of the SWPUA films. However, the cracked area was not healed, which can be seen from the optical microscopic images as shown in Fig. S6 (ESI†). A qualitative investigation of the healing ability of SWPUA-2 was carried out using an optical microscope. The big scratch on the sample almost disappears in about 330 s at a microwave power of 800 W, as shown in Fig. 6(g) and (h). Additionally, more experiments have been performed to demonstrate the self-healing ability of SWPUA-2 visually. A film was cut into three pieces and two of them were stained with malachite green and methyl red. Then, the pieces were connected and healed as shown in Fig. 6(b). The healed sample can lift a weight of 500 g and can be stretched to large deformation without any damage as shown in Fig. 6(i) and (j). Furthermore, the corresponding videos are available as ESI,† Movies S1 and S2. It is pertinent to mention that the dynamic disulfide bonds and hydrogen bonds induce good re-processability in the SWPUA films.[33] The test was performed by cutting the sample into small pieces and hot-pressing in a compression molding machine at 60 °C under the pressure of 60–80 kg cm^{-2} for 30 min without using any solvent or catalyst (Fig. 7(a) and (b)). The recovery efficiencies for the mechanical properties are shown in Fig. 7(d) and summarized in Table S6 (ESI†). After repeated reprocessing, all films exhibit acceptable tensile strength. The 1st cycle reprocessing efficiency (tensile strength) of the SWPUA films (R1 SWPUAs) varies from 77.51% to 92.57%. Furthermore, the thermal stability was also marginally improved after reprocessing as shown in Fig. 7(e). Thus, it can be concluded that the excellent self-healing ability and re-processable capability of the newly synthesized SWPUA film would prolong its

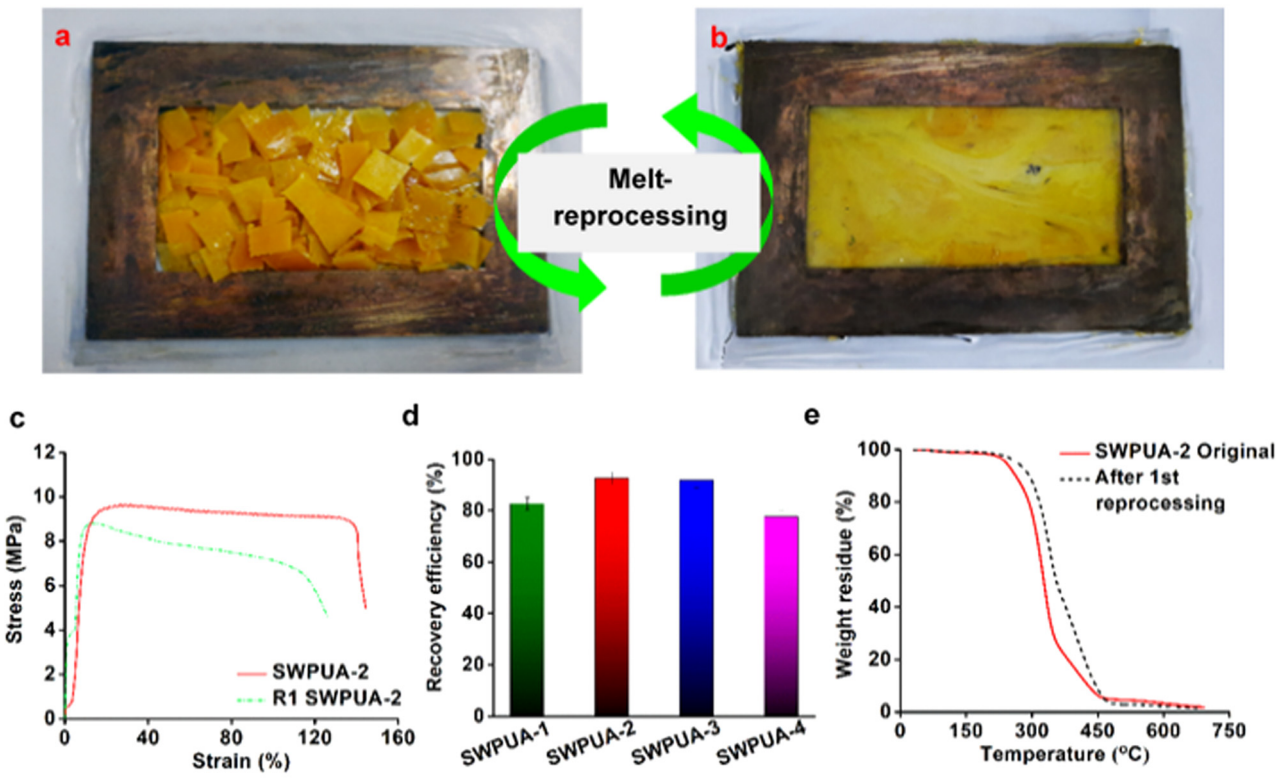

Fig. 7 (a) and (b) Digital images of the reprocessed SWPUA-2 film at 60 °C with a pressure of 60–80 kg cm^{-2} in 30 min, (c) stress–strain profiles of SWPUA-2 after the 1st cycle (R1 SWPUA-2) of reprocessing, (d) tensile strength recovery (%) of the SWPUA film after the 1st cycle of reprocessing, and (e) TGA curves of the pristine and reprocessed SWPUA-2 film.

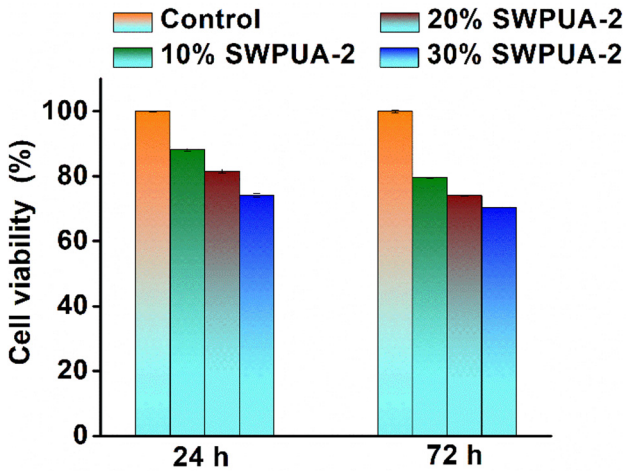

Fig. 8 Cell viability studies of L929 cells treated with different concentrations of SWPUA-2 solution (10%, 20%, 30%) after 24 h and 72 h.

service life, resulting in sustainability *via* reducing environmental pollution and raw material waste.[34]

Biocompatibility evaluation

MTT assay. The proliferation of L929 cells on three different concentrations of SWPUA-2 material was analyzed by MTT assay.[35] Fig. 8 shows that all of the concentrations indicate comparable cell proliferation to that of the tissue culture microliter plate after 24 h and 72 h of incubation. The percentages of cell viability on 10% SWPUA-2, 20% SWPUA-2, and 30% SWPUA-2 after 24 h were 88.14%, 81.52%, and 75.23%, respectively. After 72 h, they showed 79.5%, 74.07%, and 70.39% cell viability respectively. As a result, the *in vitro* cytotoxicity assays revealed that all doses of SWPUA-2 (10%, 20%, and 30%) were capable of sustaining the development of cells and did not demonstrate any cytotoxicity after three days of incubation. The results are shown as a percentage of cell proliferation at various periods in various treatment groups.

Live/dead assay. Dead cells stained with EtBr fluoresced red, whereas living cells stained with calcein AM fluoresced green. In Fig. 9(h), cells treated with 30% of SWPUA-2 solution showed a rounder shape compared to the normal fibroblast morphology due to the higher hydrophobicity of the SWPUA-2 material. However, in 10% and 20% SWPUA-2, more cells with a fibroblast morphology can be seen. These two compositions showed fewer dead cells after 3 days of cell culture. On increasing the concentration of SWPUA-2, the number of cells decreases. *In vitro*, the biocompatibility of the various concentrations of SWPUA 2 enables cellular adhesion and proliferation of L929 cells, according to investigations on cellular viability and proliferation.[36]

A UV-curable SWPUA/GelMA/gelatin-based ink for biomedical scaffold preparation

The ink composition and optimized processing parameters are mentioned in Table S8 (ESI†) and printed as model articles like a slice-cuboid and sliced-disc (Fig. 10(a)). The scaffolds were kept under UV radiation in the range of 365–410 nm after printing, with some extent of cross-linking. Then, the printed scaffolds were kept in a hot air oven for 48 h at 50 °C for drying. As shown in Fig. 10(b) and (c), the cuboid and disc scaffolds are shown to be dimensionally stable; however, as the layer height grew, the results showed decreased porosity. Movie S3 (ESI†) shows the 3D printing process.

The optimized composition of the ink demonstrated good printability showing enough scaffold height (around 5 mm) with an optimized concentration of GelMA and gelatin in the SWPUA-2. The SWPUA-2 solution showed adequate biocompatibility against L929 fibroblast cells. The other two materials, photo-cross-linkable GelMA, and gelatin, are well-known biocompatible materials that have been studied a lot in biomedical applications for tissue engineering that promote cell growth,

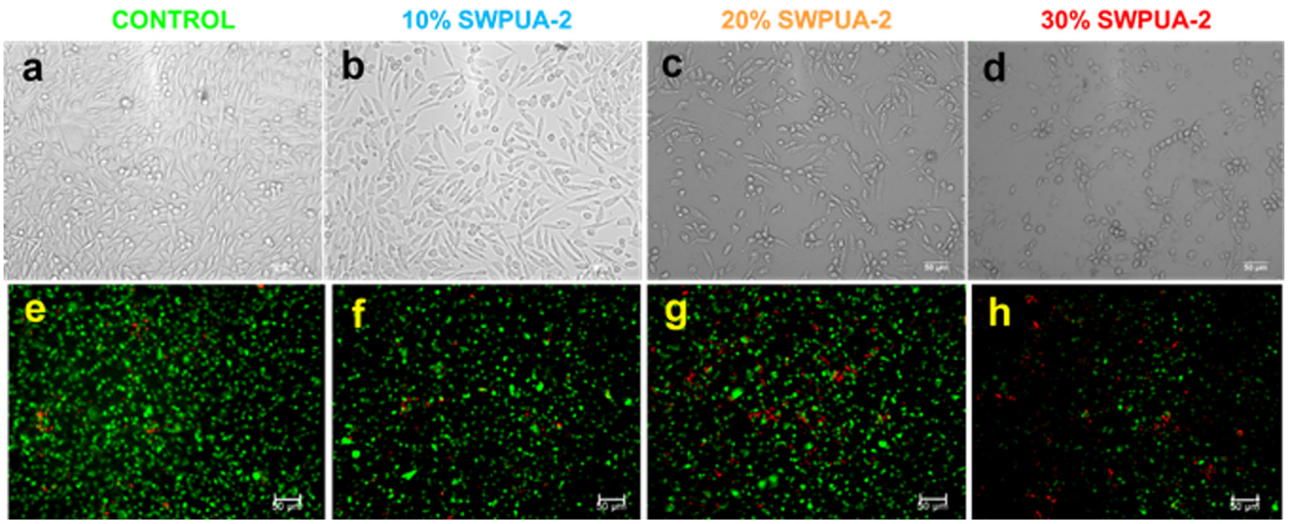

Fig. 9 (a)–(d) Bright-field micrographs and (e)–(h) live/dead staining of L929 cells treated with the control and various percentages of SWPUA-2 solution (10%, 20%, and 30%) after 3 days of incubation. (Scale bar: 50 μm).

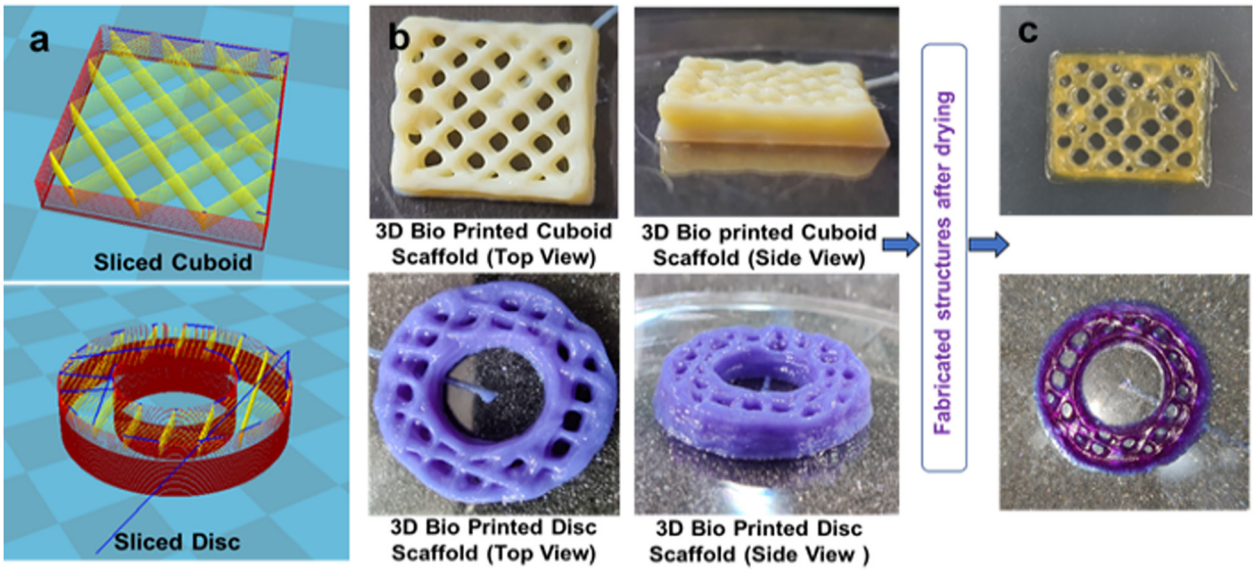

Fig. 10 (a) 3D slicing model of a cuboid and disc and (b) and (c) 3D bio-printed cuboid and disc scaffolds before and after drying.

adhesion, and function.[37] Increased layer height led to the accumulation of extruded materials at cross-sectional points, which then covered the pores, causing reduced porosity. The printed scaffold's height and material spill problem can be addressed by adding more gelatin percentage or other natural polymers, such as alginate (ionic crosslinked) and fillers, by controlling process parameters such as bed temperature, ink, and environment temperature.[38] Dried scaffolds were found to be dimensionally stable at room temperature. The GelMA/gelatin/SWPUA-2-based ink was printable, and its dried scaffolds were dimensionally stable. To improve their properties, like mechanical strength, reduced degradability, porosity, and biocompatibility, many approaches can be used, such as the incorporation of nanomaterials (nano clay and CNTs), making blends, and the use of biocompatible cross-linkers for gelatin and SWPUA-2.[39] The printed scaffolds can potentially treat articular cartilage defects by incorporating mesenchymal stem cells (MSCs) and can be used in wound healing and bone regeneration.[40]

Biodegradation of the SWPUA films

The partial biodegradability of the SWPUA films was established by plotting the weight loss percentage against time following a soil burial test. The weight loss of the buried SWPUA films was determined after 120 days. SEM images and 3D surface images (Fig. 11(a) and (d)) demonstrated the bacterial growth on the SWPUA films. The surface of the biodegraded film is craggier than the non-degraded film. The four steps that are essential for biodegradation include permeation of water molecules, hydrolysis of ester groups, solubilization of these groups, and transformation into water, CO_2, and humus by enzymes and bacteria. Some bacteria such as *Pseudomonas aeruginosa* and *Bacillus subtilis*, can easily attack the hydrolysable groups (*e.g.* ester groups of PCL, MG_{CO}, and GECA) of a PU matrix and help in the deterioration process.[41,42] Moreover, Fig. S7 (ESI†) shows that the weight loss percentage of the polymeric film increases with time. Thus, the SWPUA films prepared in this study are biodegradable in the soil environment.

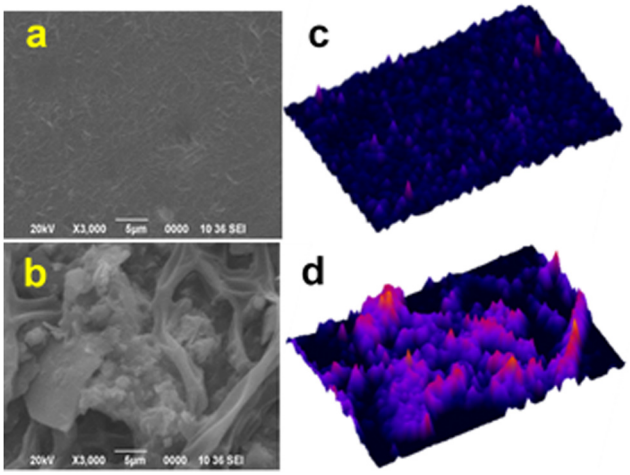

Fig. 11 (a) and (b) SEM images of controlled (un-degraded) and degraded films of SWPUA-2, respectively and (c) and (d) 3D surface plots of the SEM images obtained from ImageJ software.

Conclusion

In conclusion, based on the triple synergistic effect of a 'dynamic hard domain', 'multiple hierarchical hydrogen bonding', and 'semi-interpenetrating network (IPN) formation', a series of bio-based SWPUA dispersions were synthesized to address the dilemma that exists between high mechanical strength and good healing efficiency in a single WPU elastomer

under solvent-free and surfactant-free conditions. The synthesis process merges two polymerization mechanisms, *i.e.* step-growth and free radical chain-growth polymerizations. At the initial stage, acrylate monomers act as the diluent to reduce the viscosity of the polymerized polyurethane medium and at the final stage they are polymerized *via* seeded mini-emulsion free radical polymerization by KPS. Bis(2-aminophenyl) disulfide was introduced into the WPU matrix as the hard domain with dynamic S–S linkages to achieve optimum healing efficiency and mechanical properties. Impressively, the resulting films exhibited good mechanical robustness and thermal stability along with good self-healing ability in the presence of microwave radiation. The reversible and dynamic S–S bond and multiple hierarchical hydrogen bonds are responsible for the good healing ability. Concurrently, the rigid benzene rings and short-chain acrylate moieties enhance the ultimate tensile strength. A load of 4 kg can be lifted vertically and successfully by an SWPUA film (0.377 g), which is 10 610 times heavier than its weight. Additionally, all films are biodegradable and reprocessable under mild conditions. Most importantly, the MTT assay and live/dead assay of L929 cells on the SWPUA dispersion established its biocompatibility. Furthermore, the SWPUA/GelMA/gelatin ink can be used for developing sliced cuboid and disc scaffolds. These scaffolds have the potential for the treatment of articular cartilage defects by incorporating MSCs, in wound healing, and bone regeneration.

Author contributions

Samiran Morang: conceptualization, methodology, writing – original draft, investigation. Jay Hind Rajput: writing, investigation (3D printability). Anwesha Mukherjee: writing, investigation (bio-related work). Atharva Poundarik: supervision, validation (3D printability). Bodhisatwa Das: supervision, validation (bio-related work). Niranjan Karak: conceptualization, supervision, validation, editing, and submission.

Conflicts of interest

There are no conflicts to declare.

Acknowledgements

The authors express their gratitude to SAIC, and Advanced Functional Material Laboratory (Prof. P. Deb), Tezpur University for providing analytical support and CSIR-HRDG, India for providing a Senior Research Fellowship to SM (file no: 09/796(0115)/2020-EMR-I).

References

1 X. Zhu, K. Han, C. Li, J. Wang, J. Yuan, Z. Pan and M. Pan, *ACS Appl. Mater. Interfaces*, 2023, **15**, 19414–19426.
2 Z. W. An, R. Xue, K. Ye, H. Zhao, Y. Liu, P. Li, Z. M. Chen, C. X. Huang and G. H. Hu, *Nanoscale*, 2023, **15**, 6505–6520.
3 Y. Yang and M. W. Urban, *Chem. Soc. Rev.*, 2013, **42**, 7446–7467.
4 S. Wang and M. W. Urban, *Nat. Rev. Mater.*, 2020, **5**, 562–583.
5 S. M. Kim, H. Jeon, S. H. Shin, S. A. Park, J. Jegal, S. Y. Hwang, D. X. Oh and J. Park, *Adv. Mater.*, 2018, **30**, 1705145.
6 D. Wang, J. H. Xu, J. Y. Chen, P. Hu, Y. Wang, W. Jiang and J. J. Fu, *Adv. Funct. Mater.*, 2020, **30**, 1907109.
7 L. Zhang, Z. Liu, X. Wu, Q. Guan, S. Chen, L. Sun, Y. Guo, S. Wang, J. Song, E. M. Jeffries, C. He, F. L. Qing, X. Bao and Z. You, *Adv. Mater.*, 2019, **31**, 1901402.
8 W. Fan, Y. Jin, L. Shi, R. Zhou and W. Du, *J. Mater. Chem. A*, 2020, **8**, 6757–6767.
9 Y. Li, W. Li, A. Sun, M. Jing, X. Liu, L. Wei, K. Wu and Q. Fu, *Mater. Horiz.*, 2021, **8**, 267–275.
10 C. Zhang, H. Liang, D. Liang, Z. Lin, Q. Chen, P. Feng and Q. Wang, *Angew. Chem., Int. Ed.*, 2021, **60**, 4289.
11 Y. Zhang, Y. Wu, J. Li and K. Zhang, *Polym. Chem.*, 2021, **12**, 6161–6166.
12 F. Dong, X. Xinxin, L. Guo, Y. Wang, H. Shaghaleh, Z. Huang, X. Xu, S. Wang and H. Liu, *J. Mater. Chem. A*, 2022, **10**, 10139–10149.
13 J. Rong, J. Zhong, W. Yan, M. Liu, Y. Zhang, Y. Qiao, C. Fu, F. Gao, L. Shen and H. He, *Polymer*, 2021, **221**, 123625.
14 C. Liu, Q. Yin, Q. Yuan, L. Hao, L. Shi, Y. Bao, B. Lyu and J. Ma, *Polym. Chem.*, 2022, **13**, 5647–5658.
15 X. Wu, M. Liu, J. Zhong, Y. Zhong, J. Rong, F. Gao, Y. Qiao, L. Shen and H. He, *New J. Chem.*, 2022, **46**, 13415–13421.
16 S. Liang, P. Wang, Z. Sun, H. An, X. Wang and N. Li, *J. Appl. Polym. Sci.*, 2023, **140**, 53744.
17 S. Morang, N. Biswakarma, R. C. Deka and N. Karak, *Prog. Org. Coat.*, 2022, **168**, 106880.
18 S. Morang, A. Bandyopadhyay, B. B. Mandal and N. Karak, *ACS Appl. Bio Mater.*, 2023, **6**, 2771–2784.
19 A. I. V. D. Bulcke, B. Bogdanov, N. D. Rooze, E. H. Schacht, M. Cornelissen and H. Berghmans, *Biomacromolecules*, 2000, **1**, 31–38.
20 T. Jiang, T. Yang, Q. Bao, W. Sun, M. Yang and C. Mao, *J. Mater. Chem. B*, 2022, **10**, 4741–4758.
21 R. Chen, C. Zhang and M. R. Kessler, *RSC Adv.*, 2014, **4**, 35476–35483.
22 A. Lopez, E. Degrandi-Contraires, E. Canetta, C. Creton, J. L. Keddie and M. Asua, *Langmuir*, 2011, **27**, 3878–3888.
23 M. Li, E. S. Daniels, V. Dimonie, E. D. Sudol and M. S. El-aasser, *Macromolecules*, 2005, **38**, 4183–4192.
24 S. S. Rane and P. Choi, *Chem. Mater.*, 2005, **17**, 926.
25 S. Zhang, D. Zhang, H. Bai and W. Ming, *ACS Appl. Nano Mater.*, 2020, **3**, 59–67.
26 Z. Dai, P. Jiang, W. Lou, P. Zhang, Y. Bao and X. Gao, *Eur. Polym. J.*, 2020, **139**, 109994.
27 H. Xu, F. Qiu, Y. Wang, W. Wu, D. Yang and Q. Guo, *Prog. Org. Coat.*, 2012, **73**, 47–53.
28 S. Mehravar, N. Ballard, A. Agirre, R. Tomovska and J. M. Asua, *Macromol. Mater. Eng.*, 2019, **304**, 1–10.
29 F. Sun, L. Liu, J. Xu and J. Fu, *Mater. Chem. Front.*, 2023, **7**(17), 3494–3523, Advance Article.

30 S. Burattini, D. Chappell, H. M. Colquhoun and W. Hayes, *Chem. Soc. Rev.*, 2010, **39**, 1973–1985.
31 S. Nevejans, N. Ballard, I. Miranda, B. Reck and M. Asua, *Phys. Chem. Chem. Phys.*, 2016, **18**, 27577–27583.
32 M. Zhang, F. Zhao and Y. Luo, *ACS Omega*, 2019, **4**, 1703–1714.
33 R. Xue, H. Zhao, Z. W. An, W. Wu, Y. Jiang, P. Li, C. X. Huang, D. Shi, R. K. Li, G. H. Hu and S. F. Wang, *ACS Nano*, 2023, **17**, 5653–5662.
34 X. Xu, J. Wu, M. Li, S. Wang, H. Feng, B. Wang, K. Hu, C. Zhang, J. Zhu and S. Ma, *Polym. Chem.*, 2023, **14**, 523–532.
35 J. Xie, S. Tian, H. Zhang, C. Feng, Y. Han, H. Dai and L. Yan, *Biomacromolecules*, 2023, **24**, 2225–2236.
36 Y. Zhao, Y. Qian, H. Wang, W. Zhao, J. Zhao and H. Zhang, *ACS Appl. Polym. Mater.*, 2023, **5**, 3999–4010.
37 Y. J. Wang, U. S. Jeng and S. H. Hsu, *ACS Biomater. Sci. Eng.*, 2018, **4**, 1397–1406.
38 Q. Gao, X. Niu, L. Shao, L. Zhou, Z. Lin, A. Sun, J. Fu, Z. Chen, J. Hu, Y. Liu and Y. He, *Biofabrication*, 2019, **11**, 035006.
39 C. Yu, J. Schimelman, P. Wang, K. L. Miller, X. Ma, S. You, J. Guan, B. Sun, W. Zhu and S. Chen, *Chem. Rev.*, 2020, **120**, 10695–10743.
40 S. Ravi, L. P. Chokkakula, P. S. Giri, G. Korra, S. R. Dey and S. N. Rath, *ACS Appl. Mater. Interfaces*, 2023, **15**, 19921–19936.
41 Y. Gao, L. Sun, P. Chen, Y. Wu, Y. Liu and C. Gao, *Polym. Degrad. Stab.*, 2023, **215**, 110441.
42 M. Wang, H. Y. Liu, N. W. Ke, G. Wu, S. C. Chen and Y. Z. Wang, *J. Mater. Chem. B*, 2023, **11**, 3164–3175.